Chemical Innovation & Technology
ISSN: 3078-7351
DOI: https://doi.org/10.61784/cit3003

SYNTHESIS AND PERFORMANCE EVALUATION OF A BIS-SCHIFF BASE AMINO ACID CORROSION INHIBITOR

JiaLe Yin, XiuMei Wang*
School of Materials Science and Engineering, Shenyang Jianzhu University, Shenyang 110168, Liaoning, China.
Corresponding Author: XiuMei Wang, Email: xmwang@alum.imr.ac.cn

Abstract: This study synthesized a bis-Schiff base amino acid corrosion inhibitor (CBS) via the condensation reaction between cysteine and glutaraldehyde. The synthesis of CBS was confirmed by Fourier-transform infrared spectroscopy (FTIR). The corrosion inhibition behavior of CBS on Q235 steel in 1 M HCl solution was systematically investigated through weight loss measurements, electrochemical impedance spectroscopy (EIS), potentiodynamic polarization (PDP), and thermodynamic analysis. Weight loss results demonstrated that CBS effectively suppressed the dissolution of Q235 steel in 1 M HCl. At 303 K and a concentration of 150 mg/L, CBS achieved a corrosion inhibition efficiency of up to 94.83%. Polarization curves revealed that both anodic and cathodic branches shifted toward lower current densities upon CBS addition, classifying it as a mixed-type inhibitor. Thermodynamic analysis indicated that the adsorption of CBS on Q235 steel followed the Langmuir isotherm model, predominantly governed by chemisorption.
Keywords: Bis-Schiff base; Q235 steel; Corrosion inhibition; Temperature

1 INTRODUCTION

Q235 steel, a widely used metallic material in construction, bridges, machinery manufacturing, and transportation industries, owes its popularity to favorable mechanical properties and cost-effectiveness. However, corrosion poses significant threats during its service life. The oxidation of active atoms and electron loss at the surface degrade critical mechanical properties (e.g., strength, toughness, and plasticity) while raising risks of structural failure, environmental pollution, and economic losses [1]. Among corrosion mitigation strategies, inhibitor addition remains one of the most practical approaches [2,3]. Although amino acid-based inhibitors are environmentally benign, their limited efficiency restricts broader applications. In contrast, Schiff bases have gained prominence due to their facile synthesis, accessible raw materials, cost-effectiveness, and structural tunability through targeted functional group incorporation.
In this work, a bis-Schiff base amino acid inhibitor—cysteine-glutaraldehyde bis-Schiff base (CBS)—was synthesized via the condensation of cysteine and glutaraldehyde. The molecular structure of CBS was characterized, and its corrosion inhibition behavior for Q235 steel in 1 M HCl was evaluated using weight loss, electrochemical measurements, and thermodynamic analyses.

2 EXPERIMENTAL

2.1 Materials

Q235 steel coupons (15 mm × 15 mm × 15 mm, surface area: 13.5 cm^2) were used as test specimens. All chemicals, including cysteine, anhydrous ethanol, glutaraldehyde, NaOH, and concentrated HCl (37%), were of analytical grade and used without further purification. Corrosive media (1 M HCl) were prepared by diluting concentrated HCl with distilled water.

2.2 Synthesis of CBS

The bis-Schiff base inhibitor CBS was synthesized in the laboratory as follows:
Cysteine (20 mmol, 2.42 g) was dissolved in 20 mL of anhydrous ethanol in a 100 mL beaker under continuous stirring. Distilled water was added dropwise until complete dissolution, yielding a pale-yellow solution. Glutaraldehyde (10 mmol, 2 mL) was then added dropwise to the mixture under 60°C water bath heating. The solution gradually transitioned from pale-yellow to khaki during this process. The reaction proceeded for 4 h under constant stirring and temperature control. Post-reaction, the solvent was evaporated, and the residue was cooled to room temperature. CBS was precipitated by adding anhydrous ethanol, followed by drying and grinding to obtain a khaki powder. Figure 1 is the synthesis route of CBS.

© By the Author(s) 2025, under the CC BY-NC-ND license (http://creativecommons.org/licenses/by-nc-nd/4.0).

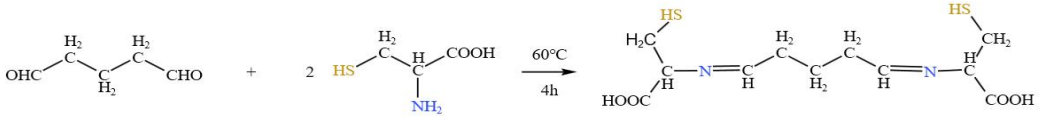


Figure 1 Synthesis Route of CBS

2.3 Weight Loss Measurements

Weight loss experiments, a widely adopted method for evaluating corrosion inhibition performance, quantify inhibitor efficiency based on mass loss of specimens before and after exposure to corrosive media. Rectangular Q235 steel coupons (surface area: 13.5 cm²) were mechanically abraded with SiC sandpapers (400#–1200#), rinsed with distilled water, degreased with acetone, and dried in a desiccator. Specimens were weighed using an analytical balance (±0.1 mg precision) and vertically suspended in 200 mL of 1 M HCl solutions (blank or containing CBS at 5, 10, 25, 50, or 150 mg/L) within 250 mL conical flasks. The flasks were maintained at controlled temperatures using a thermostatic water bath. After 4 h of immersion, specimens were removed, thoroughly rinsed with distilled water and ethanol, dried with a cold air stream, and reweighed. Three parallel experiments were conducted for each condition, and average values were calculated. The same procedure was repeated at varying temperatures (303 K, 313 K, 323 K, 333 K).
The corrosion rate (v, g·m^{-2}·h^{-1}) and inhibition efficiency (η, %) were calculated using Equations 1 and 2, respectively:

$$v = \frac{m - m_0}{A \cdot t} \tag{1}$$

Where, m and m_0 are the specimen masses (g) before and after exposure, A is the exposed surface area (m²), and t is the immersion time (h).

$$\eta = \frac{V_0 - V}{V_0} \times 100\% \tag{2}$$

Where, v_0 and v represent the corrosion rates in uninhibited and inhibited solutions, respectively.

2.4 Electrochemical Measurements

Electrochemical measurements were performed using a standard three-electrode system. A saturated calomel electrode (SCE) served as the reference electrode, a 2 cm × 2 cm platinum sheet acted as the counter electrode, and Q235 steel was employed as the working electrode. Prior to each experiment, the Q235 working electrode was mechanically ground and polished. The corrosive medium consisted of 1 M HCl solutions (blank and CBS-inhibited systems with varying inhibitor concentrations). All experiments were conducted at ambient temperature using a CHI660E electrochemical workstation.

2.4.1 Electrochemical impedance spectroscopy (EIS)

Before initiating EIS measurements, the working electrode was immersed in the test solution for at least 30 minutes to stabilize the open-circuit potential (OCP). EIS scanned from high frequency (10^5 Hz) to low frequency (0.1 Hz) with a sinusoidal perturbation amplitude of 10 mV. The obtained impedance data were fitted using ZView2 software to derive equivalent circuit parameters, generating Nyquist and Bode plots. The corrosion inhibition efficiency (η) was calculated using equation 3 as follows:

$$\eta = \frac{R_p - R_p^0}{R_p} \tag{3}$$

Where, R^0_p and R_p represent the polarization resistances (Ω·cm²) of the Q235 steel electrode in blank and CBS containing solutions, respectively.

2.4.2 Potentiodynamic polarization (PDP)

Following OCP stabilization, potentiodynamic polarization curves were recorded by scanning the potential from −0.15 V to +0.35 V relative to OCP at a scan rate of 0.0005 V/s. Experimental data were analyzed using CView software to fit polarization parameters and generate Tafel plots. The corrosion inhibition efficiency (η) was determined via equation 4 as follows:

$$\eta = \frac{I^0_{corr} - I_{corr}}{I^0_{corr}} \tag{4}$$

© By the Author(s) 2025, under the CC BY-NC-ND license (http://creativecommons.org/licenses/by-nc-nd/4.0).

Where, I^0_{corr} and I_{corr} denote the corrosion current densities (μA/cm²) for uninhibited and inhibited systems, respectively.

3 RESULTS AND DISCUSSION

3.1 Fourier-Transform Infrared Spectroscopy (FT-IR)

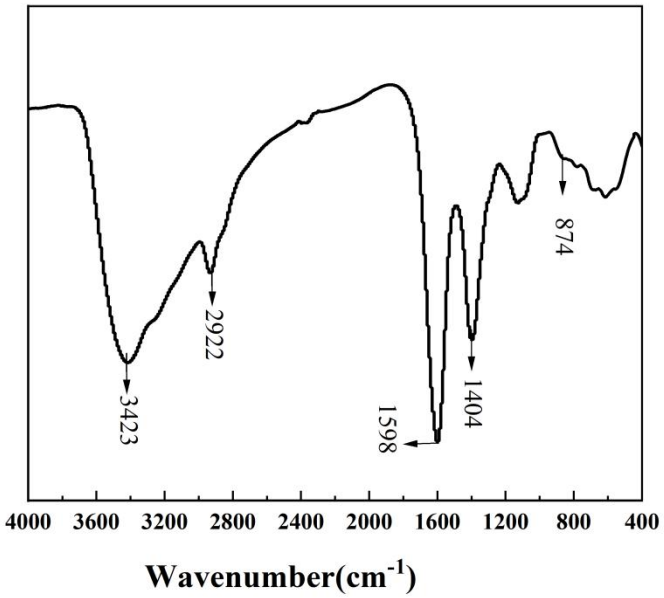


Figure 2 Infrared spectra of CBS

The FT-IR spectrum of CBS exhibited distinct absorption bands confirming its structural integrity. A prominent absorption band at 1598 cm^{-1} is attributed to the C=N stretching vibration of the imine group (– N=CH –), unambiguously confirming the successful formation of the Schiff base structure. Combined with the disappearance of the aldehyde carbonyl peak (1700 cm^{-1}) from glutaraldehyde, validate the synthesis of CBS (See Figure 2).

3.2 Weight Loss Measurements

Figures 3 and 4 illustrate the weight loss results of Q235 steel under varying temperatures (303 K, 313 K, 323 K, 333 K) and CBS inhibitor concentrations (0, 5, 10, 25, 50, 150 mg/L).

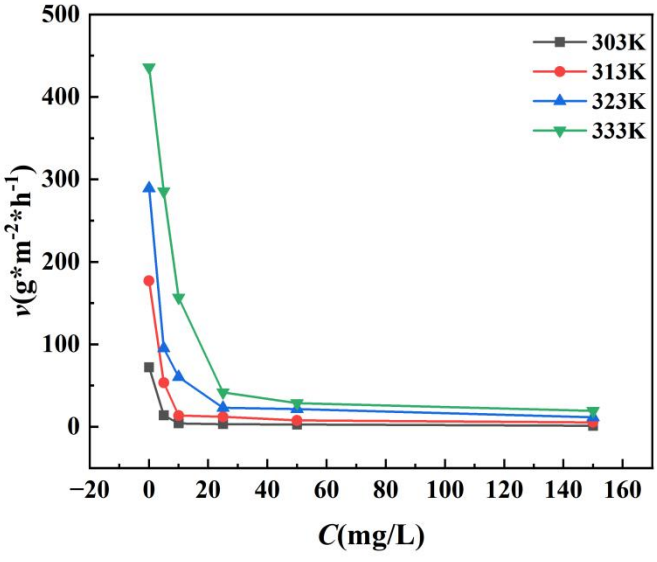


Figure 3 Influence of the concentration of CBS on the corrosion rate of Q235 steel

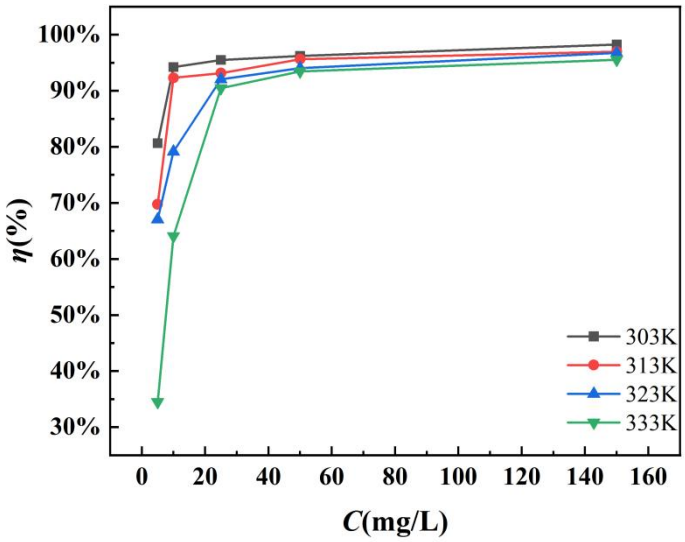


Figure 4 Influence of the Concentration of CBS on the Corrosion Inhibition Efficiency

As the seen of figure 4, within the temperature range of 303–333 K, the corrosion rate decreased progressively with increasing CBS concentration, while the inhibition efficiency showed a corresponding enhancement. At a fixed temperature, the corrosion rate declined steadily with higher CBS concentrations until reaching a plateau. Notably, within the concentration range of 50–150 mg/L, the corrosion rate and inhibition efficiency remained nearly constant. This stabilization suggests saturation of CBS adsorption on the Q235 steel surface, where inhibitor molecules form a stable protective layer. Elevating the reaction temperature significantly increased the corrosion rate and reduced inhibition efficiency. This phenomenon can be attributed to higher temperatures enhance the activity of H^+ ions in the corrosive medium, accelerating the corrosion reaction.

3.3 Electrochemical Measurements

Electrochemical tests were conducted at ambient temperature to evaluate the corrosion inhibition performance of CBS in 1 M HCl. Prior to testing, the working electrode was immersed in the solution for at least 30 minutes to stabilize the open-circuit potential (OCP). CBS concentrations ranged from 0 to 150 mg/L (0, 5, 10, 25, 50, 150 mg/L).

3.3.1 Electrochemical impedance spectroscopy (EIS)

Figures 5 and 6 present the Nyquist and Bode plots of Q235 steel in 1 M HCl without and with varying CBS concentrations, respectively.

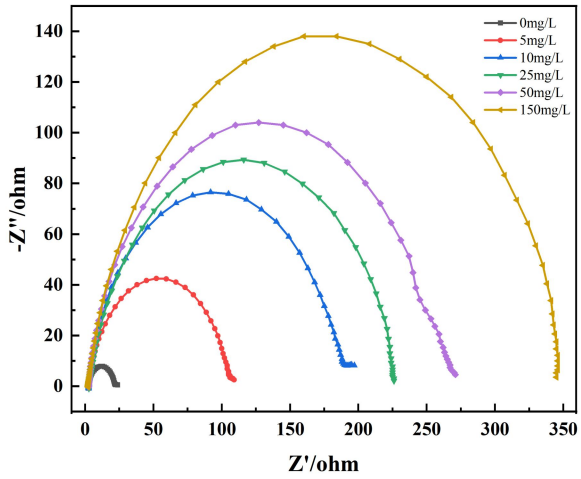


Figure 5 Nyquist Plots of Q235 Steel in 1 M HCl with Various Concentrations of CBS

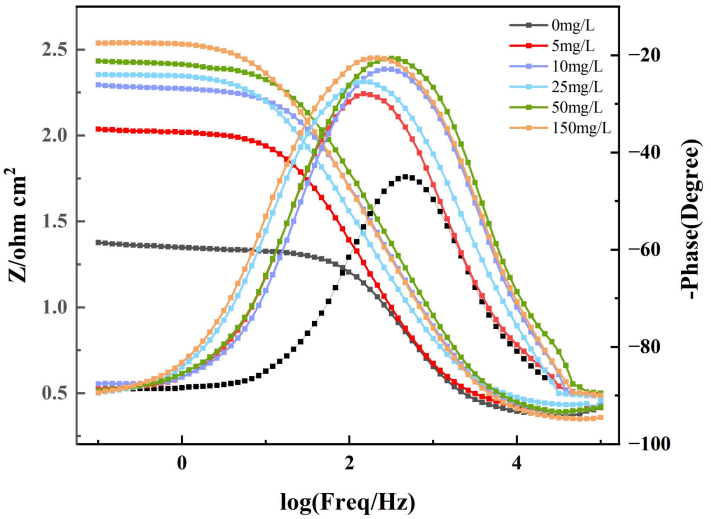


Figure 6 Bode Plots of Q235 Steel in 1 M HCl with Various Concentrations of CBS

All Nyquist plots exhibit a single semicircular capacitive loop, indicative of charge transfer-controlled corrosion at the metal-electrolyte interface [4]. The addition of CBS did not alter the shape of Nyquist or Bode plots, suggesting that CBS was not change the corrosion mechanism of steel in HCl. However, the diameter of the capacitive arcs increased with higher CBS concentrations, reflecting enhanced inhibition efficiency. This trend arises because higher CBS concentrations impede charge transfer at the steel surface, thereby suppressing corrosion [5]. The Bode plots further confirm this behavior: increased impedance modulus and phase angle with CBS addition signify reduced metal dissolution [6].

Impedance parameters were fitted using the equivalent circuit shown in Table 1 (via ZView2 software), comprising solution resistance (R_s), charge transfer resistance (R_{ct}), and a constant phase element (CPE). The fitted parameters are summarized in Table 1. Here, Y_0 represents the CPE magnitude, and n (dispersion coefficient, $0 < n < 1$) quantifies deviations from ideal capacitive behavior. Since Nyquist plots feature a single semicircle,R_{ct} corresponds to the polarization resistance (R_p).

Table 1 Electrochemical Impedance Parameters of CBS in 1 M HCl

C/(mg/L)	R_s/(Ω·cm^{-2})	Y_0/10^3(F·cm^{-2}·)	n	R_{ct}/(Ω·cm^{-2})	η/(%)
5	2.563	0.1406	0.8759	103.5	80.81
10	2.312	0.1242	0.8100	191.1	89.61
25	2.777	0.1108	0.8530	223.9	91.13
50	2.310	0.0817	0.8309	263.8	92.47
150	2.250	0.0721	0.8727	344.3	94.23

As shown in Table 1, R_{ct} values increase with CBS concentration, indicating stronger inhibition. This arises from adsorbed CBS molecules forming a protective barrier that hinders electron transfer between the steel surface and corrosive medium. Higher CBS concentrations enhance barrier integrity, aligning with weight loss results.

3.3.2 Potentiodynamic polarization (PDP)

Potentiodynamic polarization curves of Q235 steel in 1 M HCl with and without CBS are shown in Figure 7. The electrochemical parameters are listed in Table 2.

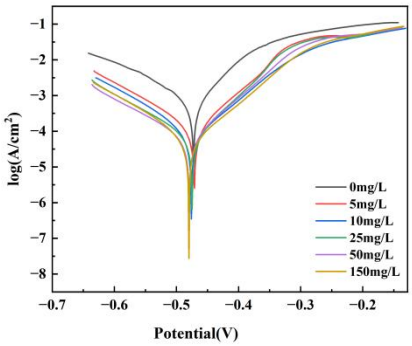


Figure 7 Polarization Curves of Q235 Steel in 1 M HCl with Various Concentrations of CBS

Table 2 Potentiodynamic Polarization Parameters of CBS in 1 M HCl

C/(mg·L^{-1})	E_{corr}(vs.SCE)/(V)	I_{corr}/(A·cm^{-2})	β_c	β_a	η/(%)
5	-0.472	1.14×10^{-4}	96.38	97.22	87.20
10	-0.476	8.37×10^{-5}	94.00	77.27	90.58
25	-0.475	7.08×10^{-5}	104.6	63.39	92.03
50	-0.479	6.68×10^{-5}	111.0	69.90	92.48
150	-0.481	5.01×10^{-5}	100.3	80.66	94.36

Both anodic and cathodic current densities decreased with CBS addition, confirming that CBS suppresses anodic metal dissolution and cathodic hydrogen reaction. A corrosion potential shift (<85 mV) classifies CBS as a mixed-type inhibitor [7]. At 150 mg/L, CBS achieves a maximum inhibition efficiency of 94.36%, demonstrating robust protection. Corrosion current densities (I_{corr}) decline with higher CBS concentrations due to the formation of an adsorbed inhibitor film, which reduces electron exchange between the metal and electrolyte. This trend aligns with weight loss measurements.

3.4 Adsorption Isotherm and Thermodynamic Parameters

Organic corrosion inhibitors typically protect metals by adsorbing onto the surface to form a stable, dense protective layer, isolating the metal from the corrosive medium. Adsorption isotherms is used to the interaction between inhibitor molecules and the metal interface, elucidating adsorption behavior and mechanisms [8].

The effectiveness of inhibitor adsorption correlates with surface coverage (θ), which varies with inhibitor concentration. Experimental data for CBS on Q235 steel in 1 M HCl were fitted to the Langmuir adsorption isotherm model using by equation 5:

$$\frac{C}{\theta}=\frac{1}{K_{ads}}+C \tag{5}$$

Where, C is the inhibitor concentration (mg/L), K_{ads} is the adsorption equilibrium constant (L/mg), and θ is the surface coverage. K_{ads} was determined from the intercept of the linear C/θ vs. C plot. The standard Gibbs free energy of adsorption (ΔG_{ads}^0) was calculated using Equation 6:

$$\Delta G_{ads}^{\ 0}=-RT\ln(55.5K_{ads}) \tag{6}$$

Here, R is the gas constant (8.314 J/mol·K), T is the absolute temperature (K), and 55.5 represents the molar concentration of water in solution.

Figure 8 displays the Langmuir adsorption isotherms for CBS on Q235 steel at different temperatures, with fitted parameters summarized in Table 3.

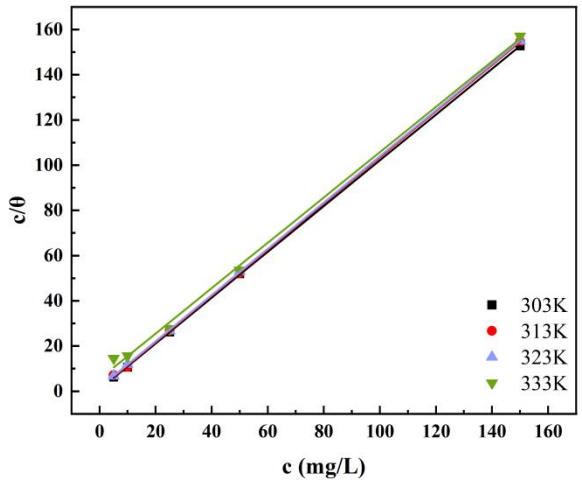


Figure 8 Langmuir Adsorption Isotherms of CBS on Q235 Steel in 1 M HCl at Varying Temperatures

Table 3 Fitted Parameters of Langmuir Adsorption Isotherms

T	R^2	K_{ads}	ΔG_{ads}^0
303.15	0.9999	1.270	-41.97
313.15	0.9999	0.780	-42.09
323.15	0.9999	0.743	-43.30
333.15	0.9972	0.165	-40.48

The linear correlation coefficients (>0.99) confirm that CBS adsorption follows the Langmuir model, implying monolayer adsorption. Increasing CBS concentrations enhance surface coverage until saturation, forming a protective film that isolates the steel from the corrosive medium. Notably, K_{ads} decreases with rising temperature (Table 3), indicating weakened adsorption capacity and reduced inhibition efficiency. This aligns with the observed increase in ΔG_{ads}^0 , signifying thermodynamically less favorable adsorption at higher temperatures.

The adsorption mechanism can be judged according to the ΔG_{ads}^0values [9,10]:

(1) $\Delta G_{ads}^0 \geq -20$kJ/mol: Physical adsorption dominates.

(2) -40kJ/mol< ΔG_{ads}^0 <-20kJ/mol: Mixed physical-chemical adsorption.

(3) $\Delta G_{ads}^0 \leq -40$kJ/mol: Chemisorption prevails.

For CBS in 1 M HCl, ΔG_{ads}^0 values range below -40 kJ/mol (303–333 K), confirming chemisorption as the primary mechanism. However, electrostatic interactions also contribute: protonated Schiff base molecules (positively charged) adsorb onto the negatively charged steel surface due to chloride ion (Cl^-) accumulation in acidic media (See Figure 9).

Adsorption thermodynamics were further analyzed using the Van't Hoff equations (7and 8):

$$\ln K = -\frac{\Delta H_{ads}^0}{RT} + \text{constant} \tag{7}$$

$$\Delta G_{ads}^0 = \Delta H_{ads}^0 - T\Delta S_{ads}^0 \tag{8}$$

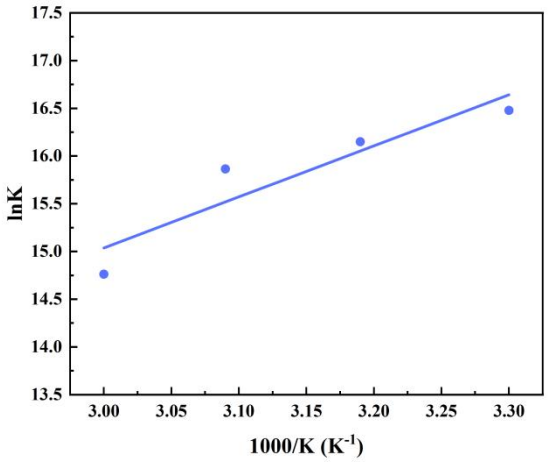


Figure 9 Van't Hoff Plot of lnK_{ads} vs. 1/T for CBS in 1 M HCl

Table 4 Thermodynamic Parameters for CBS Adsorption on Q235 Steel

ΔH_{ads}^0	ΔS_{ads}^0
-44.46	-9.67
	-7.71
	-5.70
	-10.73

The negative ΔH_{ads}^0 (Table 4) indicates an exothermic adsorption process. The slight negative ΔS_{ads}^0 suggests reduced disorder at the interface during adsorption, consistent with ordered monolayer formation.

4 CONCLUSIONS

(1) Weight loss measurements demonstrated that CBS exhibits excellent corrosion inhibition performance for Q235 steel in 1 M HCl, with inhibition efficiency increasing with CBS concentration but decreasing with temperature. At 303 K and a CBS concentration of 150 mg/L, the inhibition efficiency reached 94.83%.

(2) Electrochemical analysis revealed minimal shifts in corrosion potential (E_{corr}), while both anodic and cathodic branches of the polarization curves shifted toward lower current densities, confirming CBS as a mixed-type inhibitor. Increased capacitive arc radii in Nyquist plots, elevated impedance modulus ($|Z|$), and higher charge transfer resistance (R_{ct}) with CBS addition further validated the suppression of Q235 steel dissolution, consistent with weight loss measurements.

(3) Adsorption of CBS on Q235 steel followed the Langmuir isotherm model, dominated by chemisorption. The adsorption equilibrium constant (K_{ads}) decreased with rising temperature, indicating reduced adsorption capacity and surface coverage. Thermodynamic parameters (ΔG_{ads}^0、ΔH_{ads}^0、ΔS_{ads}^0) were all negative, signifying a spontaneous, exothermic adsorption process accompanied by entropy reduction.

COMPETING INTERESTS

The authors have no relevant financial or non-financial interests to disclose.

REFERENCES

[1] Jin Dongliang, Wang Gaofeng, Ma Xiqiang, et al. Mechanical properties of quenched low alloy medium-carbon steel. Heat Treatment of Metals, 2024, 49(2): 172-178.
[2] Qiang Y, Li H, Lan X. Self-assembling anchored film basing on two tetrazole derivatives for application to protect copper in sulfuric acid environment. Journal of Materials Science & Technology, 2020, 52:63-71.
[3] MAJDMT R M, RAMEZANZADEH B. Production of an environmentally stable anti-corrosion film based on esfand seed extract molecules-metal cations: integrated experimental and computer modeling approaches. Journal of Hazardous Materials, 2020, 382: 121029.
[4] DONG H, DING L, RAN B, et al. A study on the anti-cor-rosion mechanism of the eco-friendly inhibitor Ribavirin on Q235 steel in an acidic chloride environment. Interna-tional Journal of Electrochemical Science, 2023, 18(9): 100250.
[5] Kumar P, Soni I, Jayaprakash GK, et al. Experimental and theoretical studies of hexylmeythylimidazolium tetrafluoroborate ionic liquid as cathodic corrosion inhibitor for mild steel. Inorganic Chemistry Communications, 2022, 146: 110110.
[6] TANGM, DENG S, DU G, et al. Mikania micrantha ex-tract/KI blend as a novel synergistic inhibitor for steel corrosion in concentrated H3PO4 solution. Industrial Crops and Products, 2023, 193: 116237.
[7] Kozlica DK, Kokalj A, Milosev I. Synergistic effect of 2-mercaptobenzimidazole and octylphosphonic acid as corrosion inhibitors for copper and aluminium - An electrochemical, XPS, FTIR and DFT study. Corrosion Science, 2021, 182: 109082.
[8] Chen S, Chen S, Zhu B, et al. Magnolia grandiflora leaves extract as a novel environmentally friendly inhibitor for Q235 steel corrosion in 1 M HCl: Combining experimental and theoretical researches.Journal Of Molecular Liquids, 2020, 311: 113312
[9] Luana B F, Nascimento R C, Fábio J FS H, et al. Effects of temperature, concentration and synergism on green Schiff bases synthesized from vanillin in applications as corrosion inhibitors for carbon steel in well stimulation. Journal of Petroleum Science and Engineering, 2022, 213: 110401-110410.
[10] Chen S, Zhao H, Chen S, et al. Camphor leaves extract as a neoteric and environment friendly inhibitor for Q235 steel in HCl medium: Combining experimental and theoretical researches. Journal of Molecular Liquids, 2020, 312: 113433.